Available online at www.sciencedirect.com

ScienceDirect

IFAC PapersOnLine 58-20 (2024) 499–505

Robust Interaction using Generalized Super-Twisting Impedance Control ⋆

Jan Inge Dyrhaug [*] **Kristin Ytterstad Pettersen** [*] **Jan Tommy Gravdahl** [*]

[*] *Department of Engineering Cybernetics, Norwegian University of Science and Technology (NTNU), Trondheim, Norway (e-mail: {jan.i.dyrhaug, kristin.y.pettersen, jan.tommy.gravdahl}@ntnu.no)*

Abstract: With the goal of performing robotic intervention tasks reliably with high accuracy under uncertainty and unknown disturbances, robust control methods such as sliding mode are appealing. However, contact forces cannot be considered as disturbances in this setting and compliance to the unknown contact geometry and forces is crucial. Impedance control and passivity-based techniques can guarantee closed-loop stability when interacting with passive environments, but at the loss of precision. In this paper, we use the generalized super-twisting algorithm to obtain a controller which achieves the desired impedance even with disturbances like ocean currents and model errors. Global asymptotic stability is proved under perturbations with a bounded time derivative. The performance of the proposed super-twisting impedance control law is demonstrated in simulations of an underwater vehicle. It is compared with pure impedance control and first-order sliding mode and achieves the desired impedance with respect to the contact force despite model errors and ocean currents, with a continuous control input.

Keywords: underwater robotics, interaction, robustness, sliding mode, impedance control

1. INTRODUCTION

When robots are interacting physically with the environment, pure position control is often not a good approach. This is due to the lack of control over the interaction force. Infeasible references can then easily lead to excessively large contact forces, especially when including integral action, which is typically used to compensate for disturbances. In that case, if the reference position is inside an object, the contact force preventing further penetration, will cause the integral of the error to grow, thereby increasing the control input and the contact force until some physical limits are reached. Force control also has its limitations, however, being prone to position drift and instabilities. With the goal of robust and stable interaction, it is clear that both the position and the force need to be considered.

In our previous work (Dyrhaug et al., 2023) we showed how pure tracking control of position can be made robust and combined in a strict task-priority framework. However, when interacting with the environment, the contact force should be taken into account to ensure stable interaction.

Impedance control (Hogan, 1984) is one of the most used methods for interaction. The goal is to impose a desired dynamic relationship between the interaction variables, typically the contact force and the position/velocity. In this way, stable interaction behavior can be achieved in uncertain environments. However, in the presence of disturbances and model errors, there will be a loss of precision in both the position and force response. Moreover, the desired impedance with respect to the contact force is only attained when there are no model errors or other perturbations than the contact force. That is not the case in the underwater domain, so it is desirable to make the method more robust. If not, the degree of disturbance rejection is limited to the desired impedance. This will give insufficient disturbance rejection when there are large model uncertainties and environmental disturbances while simultaneously a compliant contact behavior is desired.

The geometry and mechanics of the task impose constraints on the possible forces and motions. It is natural to divide the task space into complementary subspaces that are either position- or force controlled. This is the framework of hybrid position/force control (Raibert and Craig, 1981). While it allows for direct force control, the method involves switching when the constraints change. Impedance control, on the other hand, does not, and we will thus use an impedance control approach in this work.

The impedance controller can be made robust by employing sliding mode techniques. Dai et al. (2020) apply the generalized impedance control to an intervention-AUV with an arm in simulation and conduct experiments with a force sensor rigidly attached to the body of the vehicle. They define the sliding variable following Chan and Chen (2001), and employ a simple first-order sliding mode controller, with a saturation function to mitigate chattering. Nicolis et al. (2020) use a different definition of the sliding surface and employ a super-twisting algorithm.

⋆ This project has received funding from the European Research Council (ERC) under the European Union's Horizon 2020 research and innovation programme, through the ERC Advanced Grant 101017697-CRÈME. The work is also supported by the Research Council of Norway through the Centres of Excellence funding scheme, project No. 223254 – NTNU AMOS.

10.1016/j.ifacol.2024.10.103

The use of a second-order sliding mode controller allows for a stronger reduction of chattering without sacrificing as much accuracy. However, the stability proof is only carried out for a first-order algorithm.

In this work, we use the sliding variable of generalized impedance control (Yao et al., 1994; Chan and Chen, 2001) which gives a flexible parametrization and does not require acceleration measurements. In order to compare the method with the pure impedance controller, we set the desired force equal to zero. We integrate this in a second-order sliding mode scheme, which, compared to Dai et al. (2020), allows for a stronger reduction of chattering without sacrificing as much accuracy. Specifically, we employ the generalized super-twisting algorithm (GSTA) (Moreno, 2009), which only requires knowledge of the sliding variable and not its time derivative, in contrast to other second-order sliding mode algorithms, and also provides a continuous control input. Moreover, we use quaternions to represent the orientation without singularities.

We present a stability analysis of the resulting closed-loop system, showing that global asymptotic stability is achieved under a large class of disturbances with bounded time derivatives. In a special case, the result is strengthened to finite-time stability. This is stronger than previous results which only showed practical stability with a continuous approximation of first-order sliding mode. The performance of the control system is evaluated in simulations of an underwater vehicle and show that the desired impedance can be achieved in the presence of significant model errors and environmental disturbances such as ocean currents.

The paper is organized as follows. First, we provide some background material on robust interaction control in Section 2. Then, we develop our proposed super-twisting impedance controller in Section 3 and apply the control method on an underwater vehicle. In Section 4, we present the stability analysis. The simulation results are presented in Section 5. Finally, in Section 6, we summarize the results and future work.

2. BACKGROUND

In this section we present some required details of existing interaction control methods to introduce the required notation and background for our approach.

2.1 Impedance control

Commonly, the desired dynamic behavior is that of a mass-spring-damper system

$$M_{\text{des}}\ddot{\tilde{x}} + D_{\text{des}}\dot{\tilde{x}} + K_{\text{des}}\tilde{x} = F_c \tag{1}$$

with $\tilde{x}$ being the position error, F_c the contact force and M_{des}, D_{des} and K_{des} representing the desired inertia, damping and stiffness, respectively. In other words, the impedance control problem can be viewed as a model following problem, where the desired impedance is achieved if the interaction variables are related by (1).

As an example of the implementation of impedance control, consider the standard manipulator equations

$$M(q)\ddot{q} + C(q,\dot{q})\dot{q} + g(q) = \tau + \tau_{\text{ext}} \tag{2}$$

where q denotes the configuration variables (typically joint angles), M is the inertia matrix, C is the Coriolis/centrifugal matrix, g denotes the gravitational torques, τ denotes the actuator output torques and $\tau_{\text{ext}} = \tau_c + \tau_{\text{dist}}$ is the sum of the contact force and disturbances. The desired impedance in the operational space is given by a dynamical relationship of the form

$$\Lambda_{\text{des}}\ddot{\tilde{x}} + D_{\text{des}}\dot{\tilde{x}} + K_{\text{des}}\tilde{x} = F_{\text{ext}}, \tag{3}$$

where $\tilde{x} = x - x_d$, $\dot{x} = J(q)\dot{q}$ and $\tau_{\text{ext}} = J^\top F_{\text{ext}}$, and in case of an invertible Jacobian J, the operational space inertia is $\Lambda = J^{-\top}MJ^{-1}$ and the Coriolis-centrifugal matrix is $\mu = J^{-\top}(C - MJ^{-1}\dot{J})J^{-1}$. Often, the desired inertia Λ_{des}, damping D_{des} and stiffness K_{des} are chosen as constant, diagonal matrices to give a decoupled response.

With the above notation, the classical impedance controller is given by (Ott, 2008, Ch. 3)

$$\begin{aligned}\tau = g(q) &+ J(q)^\top(\Lambda(x)\ddot{x}_d + \mu(x,\dot{x})\dot{x}) \\ &- J(q)^\top\Lambda(x)\Lambda_{\text{des}}^{-1}(K_{\text{des}}\tilde{x} + D_{\text{des}}\dot{\tilde{x}}) \\ &+ J(q)^\top(\Lambda(x)\Lambda_{\text{des}}^{-1} - I)F_{\text{ext}}.\end{aligned} \tag{4}$$

Note that feedback of the external force F_{ext} is needed to shape the inertia, which can be problematic in practice due to noncolocation of the sensor and the actuators, leading to delays and potentially instability issues (Hogan, 2022). In order to avoid force feedback, one can keep the natural inertia $\Lambda(x)$. Since the desired inertia matrix in this case depends on the position x, it is natural that also the desired damping should vary accordingly. A procedure for this based on the generalized eigenvalue decomposition of symmetric matrices is given in Ott (2008, Sec. 3.3). Since the dynamics in that case become coupled and nonlinear, it requires a more complicated analysis. However, in the absence of disturbances, uniform global asymptotic stability is still achieved (Ott, 2008, Sec. 3.2).

It should also be noted, that the above-mentioned controller only achieve the desired impedance with respect to the contact force when there are no model errors or other perturbations than the contact force, i.e. $\tau_{\text{ext}} = \tau_c$ in (2). That is not the case in the underwater domain, so it is desirable to make the method more robust. Otherwise, the closed loop operational space dynamics instead become

$$\Lambda_{\text{des}}\ddot{\tilde{x}} + D_{\text{des}}\dot{\tilde{x}} + K_{\text{des}}\tilde{x} = F_c + \Lambda_{\text{des}}\Lambda^{-1}F_{\text{dist}}, \tag{5}$$

where the disturbance drives the system, distorted by the ratio of desired and natural inertia, $\Lambda_{\text{des}}\Lambda^{-1}$. As noted by Dietrich and Ott (2020), this distortion can destroy dissipativity properties of for example unmodeled velocity-dependent friction and destabilize the closed-loop system.

2.2 Sliding mode impedance control

Sliding mode impedance control can be implemented with a suitable definition of the sliding surface. In Nicolis et al. (2020), an integral formulation is used to avoid the feedback of accelerations, by defining

$$\sigma = \int_{t_0}^{t}(M_{\text{des}}\ddot{\tilde{x}} + D_{\text{des}}\dot{\tilde{x}} + K_{\text{des}}\tilde{x} - F_c)d\tau \tag{6}$$

which is the integral of (1), hence the desired impedance is achieved when $\dot{\sigma} = 0$. It is therefore quite natural to employ a second-order sliding mode algorithm, which can ensure that both σ and $\dot{\sigma}$ converge to zero in finite time. However, note that $\sigma = 0$ is not required to obtain the desired dynamics (1). The use of the super-twisting algorithm will ensure that $\dot{\sigma}$ and therefore the control input is continuous, in contrast to first-order methods, in which $\dot{\sigma}$ is discontinuous.

Specifically, in this work, we will use the generalized super-twisting algorithm (GSTA) (Moreno, 2009). Compared with the standard super-twisting algorithm (Levant, 1993), the GSTA contains extra terms to counteract the effects of state-dependent perturbations that can grow exponentially in time. The super-twisting algorithm is also unique in that it only requires knowledge of the sliding variable and not its time derivative, in contrast to other second-order sliding mode controllers.

2.3 Generalized sliding mode impedance control

In order to incorporate force references, one can replace the contact force F in (6) with the force error $\tilde{F}_c = F_c - F_{c,d}$:

$$M_{\text{des}}\ddot{\tilde{x}} + D_{\text{des}}\dot{\tilde{x}} + K_{\text{des}}\tilde{x} = K_f\tilde{F}_c. \tag{7}$$

This has been called generalized impedance control (Yao et al., 1994; Chan and Chen, 2001). The effect of this is that force tracking is achieved when the position errors are zero. However, if the position references are inaccurate, the resulting force will approach the sum of the reference force and the force dictated by the stiffness K_{des} of the virtual spring. Chan and Chen (2001) also formulate a dynamic compensator (rewritten with our notation):

$$\dot{\zeta} = A\zeta + K_{pz}\tilde{x} + K_{vz}\dot{\tilde{x}} - K_{fz}\tilde{F}_c \tag{8}$$

where ζ is the state-vector of the compensator, A is any negative semi-definite matrix, and K_{pz}, K_{vz} and K_{fz} are specified so that the target model (7) is achieved in the sliding mode. The switching function is defined as

$$s = \dot{\tilde{x}} + F_1\tilde{x} + F_2\zeta \tag{9}$$

where F_1 and F_2 are constant; F_2 also being nonsingular.

This definition of the sliding variable has the advantage of more design freedom than the formulation in (6), as the matrices A, F_1 and F_2 can be tuned. Typically, however, they are chosen as diagonal. Moreover, the sliding variable does not depend directly on acceleration, even when M_{des} is not constant, and the integral of the impedance equation (7) is not forced to zero. Therefore, this is the sliding variable formulation we will use, but with $K_f = 0$ and $F_d = 0$ to compare with the pure impedance controller.

3. SUPER-TWISTING IMPEDANCE CONTROL

In this section we present our proposed control approach. The method combines the generalized impedance control concept of (7) and the sliding mode formulation of (9) with the generalized super-twisting algorithm (Moreno, 2009). To illustrate its effectiveness, we apply the method on the control of an underwater vehicle.

3.1 Dynamic model

The dynamic model of the underwater vehicle expressed in the body-frame is (Fossen, 2021, Sec. 8.1)

$$M\dot{\nu}_r + C(\nu_r)\nu_r + D(\nu_r)\nu_r + g(\eta) = \tau + \tau_c + \tau_{\text{dist}} \tag{10}$$

where $\eta = (p, q)$ is the configuration of the vehicle, consisting of the position p and orientation represented by a unit quaternion q, and $\nu = (v, \omega)$ is the linear and angular velocity of the vehicle and $\nu_r = \nu - \nu_c$ is the velocity relative to the ocean current. M is the inertia matrix, C is the Coriolis/centrifugal matrix, D is damping and g is gravitational and buoyancy forces. In more detail, M and C contain both rigid body and hydrodynamic added mass, i.e., $M = M_{\text{RB}} + M_A$ and $C = C_{\text{RB}} + C_A$. The actuator output is τ, and the contact wrench is represented with τ_c. The term τ_{dist} represents a lumped uncertainty containing matched model errors and disturbances. We will also define $\bar{\tau}_{\text{dist}}$ to be the equivalent disturbance when the effect of the ocean current is considered unknown and the model uses estimates of M, C, D and g, i.e.,

$$\begin{aligned}\bar{\tau}_{\text{dist}} = \tau_{\text{dist}} + M\dot{\nu}_c + C(\nu)\nu - C(\nu_r)\nu_r + D(\nu)\nu - D(\nu_r)\nu_r \\ + \tilde{M}\dot{\nu} + \tilde{C}(\nu)\nu + \tilde{D}(\nu)\nu + \tilde{g}(\eta)\end{aligned} \tag{11}$$

with $\tilde{x} = \hat{x} - x$ here denoting estimation errors.

3.2 Super-twisting impedance control

We will solve the following control objective:

Control problem: Design a control law $\tau(t, \eta, \nu, \tau_c)$ for (10) which despite disturbances asymptotically gives the closed-loop system the impedance defined by

$$M_d\dot{\tilde{\nu}} + D_d\tilde{\nu} + K_d\tilde{\eta} = \tau_c, \tag{12}$$

with $\tilde{\nu} = \nu - \nu_d$ and $\tilde{\eta} = (p - p_d, \tilde{q}_v)$, where $\tilde{q}_v$ is the vector part of the error quaternion $\tilde{q} = q_d^* \otimes q$. No knowledge of the current ν_c or the disturbance τ_{dist} is assumed, and only estimates of M, C, D and g. We do assume that measurements or estimations of η, ν and τ_c are available.

If we were to derive the ideal controller, similar to (4), we would choose the control law

$$\begin{aligned}\tau = M\dot{\nu}_{r,d} + C(\nu_r)\nu_r + D(\nu_r)\nu_r + g(\eta) \\ - MM_d^{-1}(K_d\tilde{\eta} + D_d\tilde{\nu}) \\ + (MM_d^{-1} - I)\tau_c - \tau_{\text{dist}}.\end{aligned} \tag{13}$$

One difference with respect to (4) is that we seek to cancel the effect of the disturbance τ_{dist} and obtain a desired impedance with respect to the contact force τ_c only. However, since the disturbance τ_{dist} and the current velocity ν_c are unknown, this control cannot be implemented. In this work, we will thus employ the generalized super-twisting algorithm (GSTA) to compensate for this disturbance.

Inspired by (9), we define the sliding variable

$$s = \tilde{\nu} + F_1\tilde{\eta} + F_2\zeta \tag{14}$$

$$\dot{\zeta} = A\zeta + K_{pz}\tilde{\eta} + K_{vz}\tilde{\nu} - K_{fz}\tau_c \tag{15}$$

with gains related by (21). Note that $\dot{\tilde{\eta}} \neq \tilde{\nu}$ because of the orientation part. For the error quaternion

$$\dot{\tilde{q}} = \begin{bmatrix} -\frac{1}{2}q_v^\top \\ \frac{1}{2}(q_w I_3 + S(q_v)) \end{bmatrix}\tilde{\omega} = T(\tilde{q})\tilde{\omega} \tag{16}$$

where q_w denotes the real part and q_v the vector part of the quaternion, and $S(\cdot)$ is the skew symmetric cross product matrix. Focusing on the vector part, we have that

$$\dot{\tilde{q}}_v = \frac{1}{2}(\tilde{q}_w I_3 + S(\tilde{q}_v))\tilde{\omega} =: U(\tilde{q})\tilde{\omega} \tag{17}$$

so

$$\dot{\tilde{\eta}} = \begin{bmatrix} \dot{\tilde{p}} \\ \dot{\tilde{q}}_v \end{bmatrix} = \begin{bmatrix} \tilde{v} \\ U(\tilde{q})\tilde{\omega} \end{bmatrix} = \begin{bmatrix} I_3 & 0_3 \\ 0_3 & U(\tilde{q}) \end{bmatrix}\tilde{\nu}. \tag{18}$$

Now, differentiating (14) we get

$$\dot{s} = \dot{\tilde{\nu}} + F_1\dot{\tilde{\eta}} + F_2\dot{\zeta} = \dot{\tilde{\nu}} + \bar{F}_1\tilde{\nu} + F_2\dot{\zeta} \tag{19}$$

with $\bar{F}_1 = F_1 \begin{bmatrix} I_3 & 0_3 \\ 0_3 & U(\tilde{q}) \end{bmatrix}$. The rest of the derivation is analogous to Chan and Chen (2001). Substituting (15) into (19) and using (14) to eliminate ζ, we get that

$$M_d\dot{\tilde{\nu}} + D_d\tilde{\nu} + K_d\tilde{\eta} = \tau_c + M_d(\dot{s} - F_2AF_2^{-1}s) \tag{20}$$

when choosing

$$K_{vz} = F_2^{-1}(M_d^{-1}D_d - \bar{F}_1 + F_2AF_2^{-1}) \tag{21a}$$
$$K_{pz} = F_2^{-1}(M_d^{-1}K_d + F_2AF_2^{-1}F_1) \tag{21b}$$
$$K_{fz} = F_2^{-1}M_d^{-1}. \tag{21c}$$

We then use a second-order sliding mode controller to enforce the desired impedance robustly. The total control of the super-twisting impedance controller is

$$\tau_{\text{GSTA-IC}} = \tau_{\text{nom}} + \hat{M}(\tau_{\text{GSTA}}(s,z) - F_2AF_2^{-1}s) \tag{22}$$

where the nominal control is

$$\tau_{\text{nom}} = \hat{M}\dot{\nu}_d + \hat{C}(\nu)\nu + \hat{D}(\nu)\nu + \hat{g}(\eta) + (\hat{M}M_d^{-1} - I)\tau_c - \hat{M}M_d^{-1}(K_d\tilde{\eta} + D_d\tilde{\nu}) \tag{23}$$

and the sliding mode part is

$$\tau_{\text{GSTA}}(s,z) = -k_1\phi_1(s) + z \tag{24a}$$
$$\dot{z} = -k_2\phi_2(s) \tag{24b}$$

where $\phi_1(s) = \lceil s \rfloor^{\frac{1}{2}} + \beta s$ and $\phi_2(s) = \frac{1}{2}\lceil s \rfloor^0 + \frac{3}{2}\beta\lceil s \rfloor^{\frac{1}{2}} + \beta^2 s$ using the short-hand notation $\lceil a \rfloor^b = |a|^b \operatorname{sgn}(a)$, with all functions evaluated element-wise. The desired wrench is mapped to the thruster inputs by

$$u = B^\dagger\tau \tag{25}$$

where B is the thruster allocation matrix and † denotes the Moore–Penrose pseudoinverse.

4. STABILITY ANALYSIS

Inserting the controller (22) into the dynamics (10), one obtains the following closed-loop dynamics:

$$\dot{\tilde{\nu}} + M_d^{-1}(D_d\tilde{\nu} + K_d\tilde{\eta} - \tau_c) = \tau_{\text{GSTA}} - F_2AF_2^{-1}s + \hat{M}^{-1}\bar{\tau}_{\text{dist}}. \tag{26}$$

Using (20) we get that

$$\dot{s} = \tau_{\text{GSTA}}(s,z) + \hat{M}^{-1}\bar{\tau}_{\text{dist}}. \tag{27}$$

Defining $\varphi = \hat{M}^{-1}\bar{\tau}_{\text{dist}}$, this equation can be written component-wise as

$$\dot{s}_i = -k_1\phi_1(s_i) + z_i + \varphi_i \tag{28}$$

which is a special case of the setting considered by (López-Caamal and Moreno, 2019, Theorem 1). Following their notation using superscripts as indexes, splitting the perturbation into a vanishing part φ^1 and a remainder φ^2, and defining $z^1 := s$ and $z^2 := z + \varphi^2$, our closed-loop system can be written as

$$\frac{d}{dt}z^1 = -K^1\phi^1(z^1) + z^2(t) + \rho^1(t, z^1, z^2) \tag{29a}$$
$$\frac{d}{dt}z^2 = -K^2\phi^2(z^1) + \rho^2(t, z^1) \tag{29b}$$

with $\rho^1 = \varphi^1$ and $\rho^2 = \dot{\varphi}^2$. Note that $(s, \dot{s}) \to (0,0)$ is implied by $(z^1, z^2) \to (0,0)$, since $\phi^1(0) = 0$ and ρ^1 vanishes when $z^1 = z^2 = 0$.

The first three assumptions of (López-Caamal and Moreno, 2019, Theorem 1) are satisfied with our choice of the functions ϕ^1 and ϕ^2, and assumption four is fulfilled since in our case $K^1 = k_1I$ and $K^2 = k_2I$ are chosen as diagonal matrices and J is diagonal. The last assumption is on the perturbations, and assumes that they can be written in terms of $\phi^1(z^1)$ and z^2 as

$$\rho^1(t, z^1, z^2) = G^1(t)\phi^1(z^1) + G^3(t)z^2 \tag{30a}$$
$$\rho^2(t, z^1) = G^2(t)\phi^2(z^1) \tag{30b}$$

where the matrices G^i are bounded. Note that our $\phi^2(s)$ contains the term $\lceil s \rfloor^0 = \operatorname{sgn}(s)$, which is able to compensate for nonvanishing perturbations ρ^2. Since the highest-order term in $\phi^2(s)$ is linear, even perturbations φ^2 with a time derivative that is linear in s can be handled. Looking at the expression (11) we see that the highest order term in ν is of second order, with quadratic damping.

With the knowledge of bounds on the elements of G^i, one can design gains K^i that render the origin of (29) stable. In particular, if the matrices G^i are diagonal, (López-Caamal and Moreno, 2019, Corollary 1) gives simple conditions for robust finite-time stability. The results of the above are summarized in the following proposition:

Proposition 1. Consider the closed-loop system (29) given by the dynamics (10) and the controller (22). Given that the perturbation ρ is bounded as described in (30), there exist gains k_1, k_2 such that $(z^1, z^2) = (0,0)$ is a globally asymptotically stable equilibrium point of (29), and $(s, \dot{s})$ thus converge asymptotically to $(0,0)$. If, moreover, the matrices G^i of (30) are diagonal, and the gains are chosen according to (López-Caamal and Moreno, 2019, Algorithm 1), the the origin $(z^1, z^2) = (0,0)$ is finite-time stable and $(s, \dot{s})$ thus converge to $(0,0)$ in finite time.

5. SIMULATIONS

In this section we will perform a simulation study to investigate the performance of the generalized super-twisting impedance controller (22-24) proposed in Section 3. Furthermore, we will compare it to the performance of a pure impedance controller, as given in (23), and with a first-order sliding mode impedance controller

$$\tau_{\text{FOSM-IC}} = \tau_{\text{nom}} - \hat{M}K_s \operatorname{sat}(s/\epsilon) \tag{31}$$

with τ_{nom} given by (23), the sliding variable s given by (14) and $\operatorname{sat}(\cdot)$ being the element-wise saturation function

$$\operatorname{sat}(x) = \begin{cases} x & \text{if } |x| < 1 \\ \operatorname{sgn}(x) & \text{if } |x| \geq 1. \end{cases} \tag{32}$$

The simulation was conducted using a model implemented in MATLAB/Simulink, using `ode1` with a fixed time step of 0.0001 due to the rapid switching in the sliding mode controller. The intervention task is to make contact and push on a wall, which is located at $x = x_c = 1$ with $k_c = 100{,}000$ N/m. The vehicle starts at rest at the origin, with no rotation. The position reference trajectory is a step from 0 to 1.01 m at $t = 1$ s, smoothed with a third-order lowpass filter with cutoff frequency $\omega_n = 2$, so that the desired acceleration becomes continuous. This deviation emulates an uncertainty in the position of the wall, in addition to producing a certain force when in contact. The orientation reference was set to $q_d = (1\ 0\ 0\ 0)$, which was

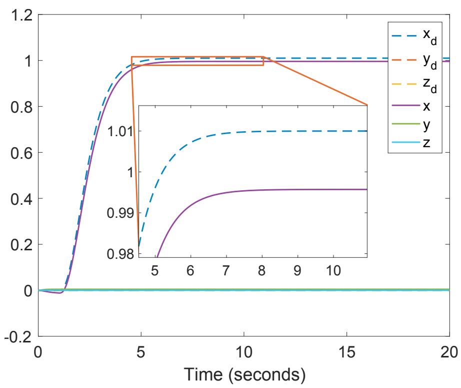

Fig. 1. Position trajectory with pure impedance control.

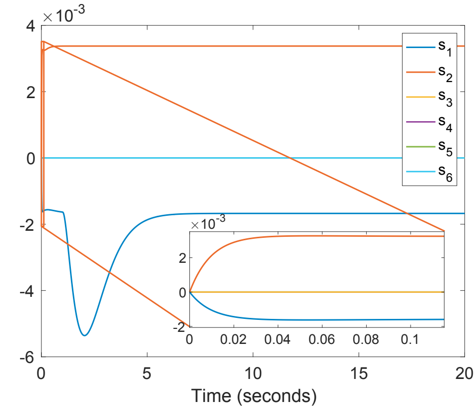

Fig. 2. Sliding variable with pure impedance control.

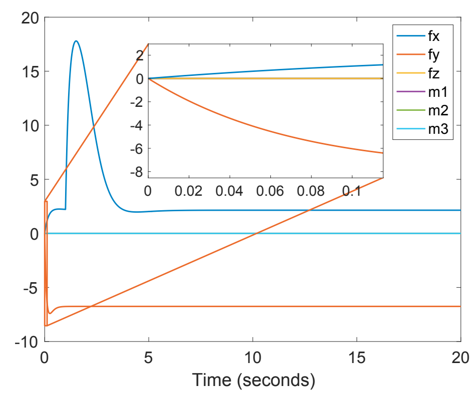

Fig. 3. Actuation force τ with pure impedance control.

also the initial orientation. The parameters of the sliding variable were chosen as $A = -100I$, $F_1 = F_2 = I$ and $K_f = I$ and the desired impedance parameters were $M_d = M$, $K_d = \text{diag}(150, 1500, 1500, 50, 50, 50)$ and D_d from the procedure given in (Ott, 2008, Sec. 3.3) and mentioned in Sec. 2.1. Together, this gives an expected stationary value of 1.5 N for the contact force. The vehicle is subjected to a constant irrotational current, $v_c = V_c\,[\cos(\beta_c)\ \sin(\beta_c)\ 0]^\top$ in the world frame, with $V_c = 0.5$ m/s and $\beta_c = 2\pi/3$, pushing the vehicle away from the wall and to the left. The GSTA parameters were set to $k_1 = 5$, $k_2 = 10$ and $\beta = 5$. The parameters of the first-order sliding mode controller (31) were set to $K_s = 19$ and $\epsilon = 10^{-3}$.

5.1 Hydrodynamic parameters and contact modeling

The hydrodynamic parameters used were identified from experiments on a BlueROV1 (Sandøy, 2016, Sec. 4.2.3), see Table A. The mass was 7.31 kg, the inertia dyadic was implemented as $I_b^b = 0.16 I_3$ and the vector from the center of the body frame to the center of gravity was $r_{bg}^b = (0,\ 0,\ 0.00019)$ m. Under the assumption that the vehicle has starboard-port symmetry with $y_g = 0$ and $I_{xy} = I_{yz} = 0$, the inertia matrix has a special structure, see (Fossen, 2021, Eq. 8.8). The Coriolis/centrifugal matrix was parametrized independently of the linear velocity v according to Fossen (2021, Eq. 3.63). The damping matrix was implemented as (Fossen, 2021, Eq 8.10)

$$D(\nu_r) = -\,\text{diag}(X_u + X_{uu}|u_r|, Y_v + Y_{vv}|v_r|, Z_w + Z_{ww}|w_r|,\\ K_p + K_{pp}|p|, M_q + M_{qq}|q|, N_r + N_{rr}|r|). \quad (33)$$

The contact force was modeled as a stiff linear spring along the x-axis, i.e.

$$F_{c,x} = \begin{cases} -k_c(x - x_c) & \text{if } x > x_c \\ 0 & \text{otherwise} \end{cases} \quad (34)$$

with the rest of the components of τ_c equal to zero.

5.2 Simulation results

We start by presenting the simulation results with the pure impedance controller (23), followed by the first-order sliding mode impedance controller (31) and finally the proposed super-twisting impedance controller (22) to illustrate how the different elements of the proposed control law act to achieve both robustness and compliance.

Figures 1-3 show the simulation results with the impedance controller (23). As Fig. 1 shows, the impedance controller is not able to fully compensate for the unknown current and does not quite reach the wall, even though the reference goes slightly into it. Contact is thus not established, due to the unknown current, whereas the expected stationary value of the contact force is 1.5 N, with a desired stiffness K_d of 150 N/m in the x-direction and a 0.01 m position error. Obviously, moving the reference further into the wall or increasing the stiffness in the x-direction would establish contact, but it would need to be tuned depending on the stiffness of the environment and the amount of disturbance, which may vary over time.

We then performed simulations with the first-order sliding mode impedance control (FOSMC) (31). Figures 4 and 5 show that contact is now achieved with a force of almost 1.5 N, but the desired impedance is still not achieved exactly (Fig. 6), as expected because of the boundary layer. Notice also that the sliding variable is well inside the boundary layer at all times, and Fig. 7 shows the actuation force, which therefore does not chatter, except for an initial transient. However, making the boundary layer ϵ smaller or increasing the control gain K_s induces severe chattering.

The GSTA controller (22-24), on the other hand, handles the unknown ocean current nicely and achieves the desired impedance, as can be seen from Fig. 9 where the contact force stabilizes at the expected value of 1.5 N, in accordance with the imposed impedance relation. As can be seen by comparing Fig. 11 with Fig. 3, the sliding mode controller expectedly uses more control effort than

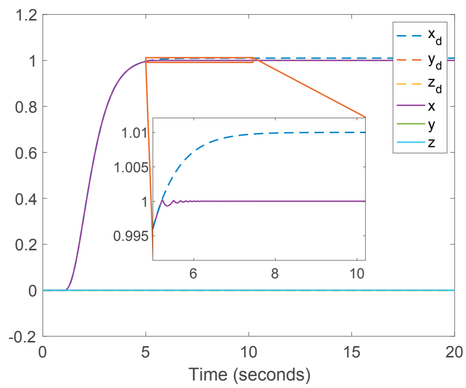

Fig. 4. Position trajectory with the first-order sliding mode impedance control.

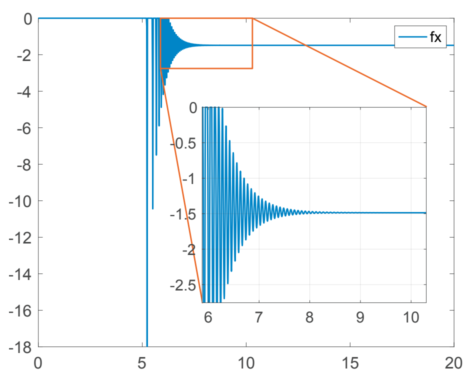

Fig. 5. Contact force trajectory with first-order sliding mode impedance control.

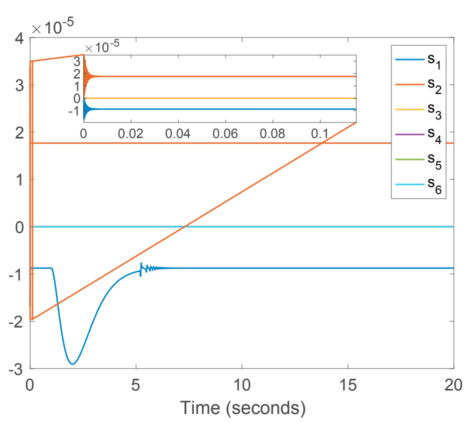

Fig. 6. Sliding variable with first-order sliding mode impedance control.

the pure impedance controller, but there is not much chattering. Compared with the FOSMC (Fig. 7), the GSTA obtains much stronger robustness with a similar control effort, and with less chattering. This is most visible in the short initial transient in the inset zoom, where the GSTA gives a continuous control and the FOSMC switches rapidly during the first fraction of a second. The difference is also clear from the sliding variable, Figs. 6 and 10.

To test the robustness further, the same case was run without the nominal control (23), that is, with only the GSTA term. Still, the controller manages to compensate for the disturbances and enforce the desired impedance.

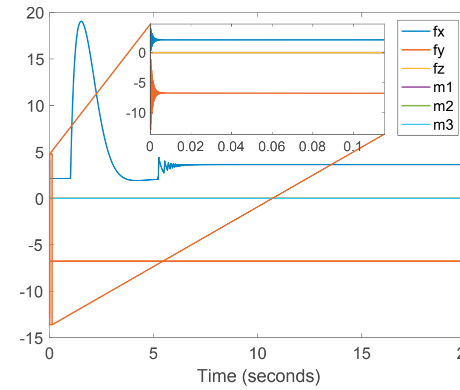

Fig. 7. Actuation force τ with first-order sliding mode impedance control.

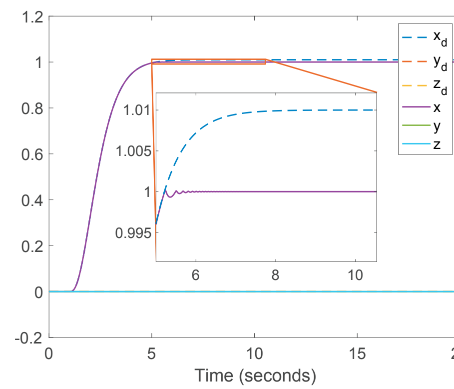

Fig. 8. Position trajectory with super-twisting impedance control.

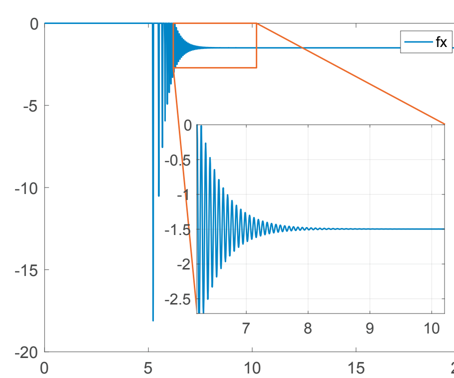

Fig. 9. Contact force trajectory with super-twisting impedance control.

As Fig. 11 shows, the actuator output is virtually identical to the that of the full controller including (23). However, due to the lack of the nominal control, the sliding mode term needs to compensate more, as we do not utilize the knowledge of the system dynamics. This is evident from Fig. 12 which shows the increased size of the integral term.

6. CONCLUSIONS AND FUTURE WORK

In this paper, we considered the problem of achieving robustness while also achieving compliant contact behavior for interaction operations. To this end, we proposed an approach where we combine generalized impedance control with the generalized super-twisting algorithm. Stability of the closed-loop system was analyzed and global asymptotic

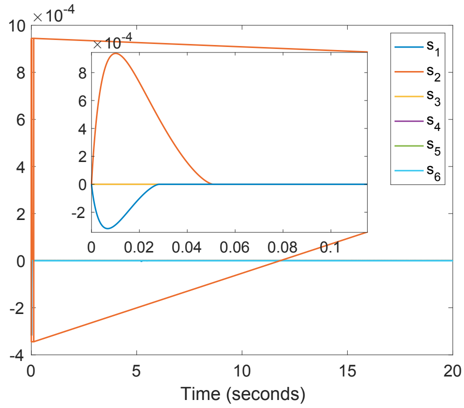

Fig. 10. Sliding variable with super-twisting impedance control.

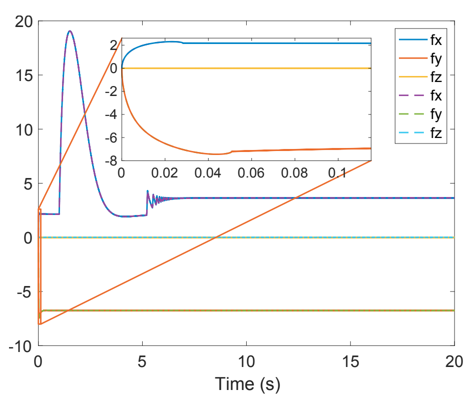

Fig. 11. Actuation force τ with super-twisting impedance control. With nominal control in solid line and without nominal control in dashed line.

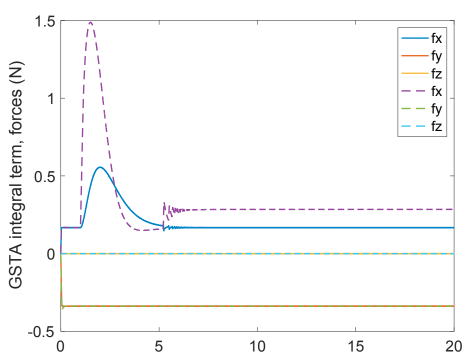

Fig. 12. Comparison of the force part of the GSTA integral term. With nominal control in solid line and without nominal control in dashed line.

stability was proved for a large class of disturbances with bounded time derivatives. The result was strengthened to finite-time stability with stronger assumptions on the disturbance. The resulting control law was applied to an underwater vehicle and tested in a simulation study. The simulations showed that the proposed controller provides good robustness properties with regard to unknown disturbances like ocean currents, while remaining compliant to the contact force. Moreover, the control input is continuous, and chattering is reduced significantly compared to the first-order sliding mode, without having to tune a boundary layer and give up some robustness. In future works, the method is to be tested in experiments to further investigate its practicality.

Appendix A. HYDRODYNAMIC PARAMETERS

Symbol	Value	Symbol	Value	Symbol	Value
$X_{\dot{u}}$	-5.5	X_u	-4.03	X_{uu}	-18.18
$Y_{\dot{v}}$	-12.7	Y_v	-6.22	Y_{vv}	-21.66
$Z_{\dot{w}}$	-14.57	Z_w	-5.18	Z_{ww}	-36.99
$K_{\dot{p}}$	-0.12	K_p	-0.07	K_{pp}	-1.55
$M_{\dot{q}}$	-0.12	M_q	-0.07	M_{qq}	-1.55
$N_{\dot{r}}$	-0.12	N_r	-0.07	N_{rr}	-1.55

REFERENCES

Chan, S. and Chen, H. (2001). Robust implementation of generalized impedance control for robot manipulators. *Advanced Robotics*, 15(6), 641–661.

Dai, P., Lu, W., Le, K., and Liu, D. (2020). Sliding Mode Impedance Control for contact intervention of an I-AUV: Simulation and experimental validation. *Ocean Engineering*, 196, 106855.

Dietrich, A. and Ott, C. (2020). Hierarchical Impedance-Based Tracking Control of Kinematically Redundant Robots. *IEEE Trans. on Robotics*, 36(1), 204–221.

Dyrhaug, J.I., Tveter, E., Schmidt-Didlaukies, H.M., Basso, E.A., Pettersen, K.Y., and Gravdahl, J.T. (2023). Robust Hierarchical Tracking Control of Vehicle-Manipulator Systems. *IFAC-PapersOnLine*, 56(2), 6696–6702.

Fossen, T.I. (2021). *Handbook of Marine Craft Hydrodynamics and Motion Control*. Wiley, 2nd edition.

Hogan, N. (1984). Impedance Control: An Approach to Manipulation. In *American Control Conf.*, 304–313.

Hogan, N. (2022). Contact and Physical Interaction. *Annual Review of Control, Robotics, and Autonomous Systems*, 5(1), 179–203.

Levant, A. (1993). Sliding order and sliding accuracy in sliding mode control. *Int. J. of Control*, 58(6), 1247–1263.

López-Caamal, F. and Moreno, J.A. (2019). Generalised multivariable supertwisting algorithm. *Int. J. of Robust and Nonlinear Control*, 29(3), 634–660.

Moreno, J.A. (2009). A linear framework for the robust stability analysis of a Generalized Super-Twisting Algorithm. In *Proc. 6th Int. Conf. on Electrical Engineering, Computing Science and Automatic Control (CCE)*.

Nicolis, D., Allevi, F., and Rocco, P. (2020). Operational Space Model Predictive Sliding Mode Control for Redundant Manipulators. *IEEE Transactions on Robotics*, 36(4), 1348–1355.

Ott, C. (2008). Cartesian Impedance Control: The Rigid Body Case. In C. Ott (ed.), *Cartesian Impedance Control of Redundant and Flexible-Joint Robots*, Tracts in Adv. Robotics, 29–44. Springer, Berlin, Heidelberg.

Raibert, M.H. and Craig, J.J. (1981). Hybrid Position/Force Control of Manipulators. *J. of Dynamic Systems, Measurement, and Control*, 103(2), 126–133.

Sandøy, S.S. (2016). *System Identification and State Estimation for ROV uDrone*. Master's thesis, NTNU.

Yao, B., Chan, S., and Wang, D. (1994). Unified formulation of variable structure control schemes for robot manipulators. *IEEE Transactions on Automatic Control*, 39(2), 371–376.